# Are Pretreatment $^{18}$F-FDG PET Tumor Textural Features in Non–Small Cell Lung Cancer Associated with Response and Survival After Chemoradiotherapy?

Gary J.R. Cook[1], Connie Yip[2], Muhammad Siddique[1], Vicky Goh[1], Sugama Chicklore[3], Arunabha Roy[1], Paul Marsden[1], Shahreen Ahmad[2], and David Landau[2]

[1]Division of Imaging Sciences and Biomedical Engineering, Kings College London, London, United Kingdom; [2]Department of Oncology, Guys and St. Thomas' NHS Foundation Trust, London, United Kingdom; and [3]Department of Nuclear Medicine, Guys and St. Thomas' NHS Foundation Trust, London, United Kingdom

There is evidence in some solid tumors that textural features of tumoral uptake in $^{18}$F-FDG PET images are associated with response to chemoradiotherapy and survival. We have investigated whether a similar relationship exists in non–small cell lung cancer (NSCLC). **Methods:** Fifty-three patients (mean age, 65.8 y; 31 men, 22 women) with NSCLC treated with chemoradiotherapy underwent pretreatment $^{18}$F-FDG PET/CT scans. Response was assessed by CT Response Evaluation Criteria in Solid Tumors (RECIST) at 12 wk. Overall survival (OS), progression-free survival (PFS), and local PFS (LPFS) were recorded. Primary tumor texture was measured by the parameters coarseness, contrast, busyness, and complexity. The following parameters were also derived from the PET data: primary tumor standardized uptake values (SUVs) (mean SUV, maximum SUV, and peak SUV), metabolic tumor volume, and total lesion glycolysis. **Results:** Compared with nonresponders, RECIST responders showed lower coarseness (mean, 0.012 vs. 0.027; $P$ = 0.004) and higher contrast (mean, 0.11 vs. 0.044; $P$ = 0.002) and busyness (mean, 0.76 vs. 0.37; $P$ = 0.027). Neither complexity nor any of the SUV parameters predicted RECIST response. By Kaplan–Meier analysis, OS, PFS, and LPFS were lower in patients with high primary tumor coarseness (median, 21.1 mo vs. not reached, $P$ = 0.003; 12.6 vs. 25.8 mo, $P$ = 0.002; and 12.9 vs. 20.5 mo, $P$ = 0.016, respectively). Tumor coarseness was an independent predictor of OS on multivariable analysis. Contrast and busyness did not show significant associations with OS ($P$ = 0.075 and 0.059, respectively), but PFS and LPFS were longer in patients with high levels of each (for contrast: median of 20.5 vs. 12.6 mo, $P$ = 0.015, and median not reached vs. 24 mo, $P$ = 0.02; and for busyness: median of 20.5 vs. 12.6 mo, $P$ = 0.01, and median not reached vs. 24 mo, $P$ = 0.006). Neither complexity nor any of the SUV parameters showed significant associations with the survival parameters. **Conclusion:** In NSCLC, baseline $^{18}$F-FDG PET scan uptake showing abnormal texture as measured by coarseness, contrast, and busyness is associated with nonresponse to chemoradiotherapy by RECIST and with poorer prognosis. Measurement of tumor metabolic heterogeneity with these parameters may provide indices that can be used to stratify patients in clinical trials for lung cancer chemoradiotherapy.

**Key Words:** non–small cell lung cancer; chemoradiotherapy; $^{18}$F-FDG PET/CT; textural analysis

Personalized medicine is a goal in modern cancer therapy, with the aim that optimal treatment can be selected for an individual patient depending on tumor characteristics in that individual. The ability to predict the behavior of a tumor to treatment before therapy is started would be invaluable in enabling stratification in clinical trials or personalizing future cancer treatments in the clinic.

In clinical routine and, increasingly, in clinical trials, serial $^{18}$F-FDG PET/CT is being used successfully in several cancers to detect early treatment effects before morphologic changes can be seen on CT or MRI. However, it has been harder to demonstrate the ability to predict response to treatment or to predict survival from a single baseline scan before therapy has been started.

In non–small cell lung cancer (NSCLC), several studies have shown the utility of serial $^{18}$F-FDG PET/CT to measure response to neoadjuvant chemotherapy (1–6), chemoradiotherapy (7,8), or novel biologic therapies (9,10). There is also more limited evidence that the level of uptake on pretreatment scans, as measured by various standardized uptake value (SUV) parameters, may be predictive (11–14), but results conflict as to whether high or low SUVs are predictive depending on treatment modality (13,14).

Beyond the relatively simple measurements of the level of tumor uptake or size, there is increasing recognition that measurement of the spatial heterogeneity of $^{18}$F-FDG PET image characteristics can give predictive information on baseline, pretherapy, imaging in several solid tumors

including sarcoma (*15*), head and neck and cervix tumors (*16–18*), and esophageal carcinoma (*19*). In NSCLC, a potential heterogeneity parameter using SUV volume histograms has been described but not clinically tested (*20*). Multimodality image feature modeling including $^{18}$F-FDG PET and CT has also been described as a possible predictor of locoregional recurrence in NSCLC after radiotherapy (*21*).

Several different textural parameters have been reported in $^{18}$F-FDG PET, but parameters derived from neighborhood gray-tone (intensity) difference matrices (NGTDM), describing features such as coarseness, contrast, busyness, and complexity (*22*), have shown the ability to differentiate primary and nodal tumor from normal tissue in head and neck cancer (*17*) and allow the delineation of radiotherapy plans (*18*). In addition, coarseness has been reported as one of the textural parameters that can predict response to chemoradiotherapy in esophageal cancer (*19*).

We hypothesized that the textural features derived from NGTDMs that reflect differences between the intensity of each voxel and its neighboring voxels in $^{18}$F-FDG PET images may be associated with differences in response to treatment and survival in NSCLC. The aim of this study was to assess the predictive and prognostic value of these parameters in patients with NSCLC being treated with concurrent chemoradiotherapy, compared with SUV parameters such as mean SUV (SUVmean), maximum SUV (SUVmax), and peak SUV (SUVpeak); metabolic tumor volume (MTV); and total lesional glycolysis (TLG).

## MATERIALS AND METHODS

A waiver of institutional review board approval was obtained for this retrospective analysis. Fifty-three consecutive patients (mean age, 65.8 y; 31 men, 22 women) with NSCLC who were treated with definitive radiotherapy and concurrent chemotherapy in our tertiary cancer center between January 2007 and December 2009 were included. All patients who were considered for definitive treatment in our center were staged with $^{18}$F-FDG PET/CT. $^{18}$F-FDG PET/CT was performed at a median of 45 d (mean, 53 d; range, 0–174 d; 25th percentile, 35 d; 75th percentile, 63 d) before treatment. There were 21 patients with adenocarcinoma, 24 with squamous cell carcinoma, and 8 for whom histologic results were not available. Clinical staging was as follows: stage 1B (*n* = 3), stage 2B (*n* = 5), stage 3A (*n* = 24), and stage 3B (*n* = 21) (*23*). No patient had metastatic M1 disease. Thus, most patients had locally advanced (stage 3) lung cancer and were not considered suitable for surgery or were medically inoperable. Clinical follow-up after treatment was performed according to departmental protocol: every 4 wk for the first 3 mo, every 2 mo for the first year, and every 3 mo thereafter.

Patients were treated with 64 Gy of radiotherapy and concurrent vincristine–cisplatin or vincristine–carboplatin chemotherapy. Patient response was assessed with Response Evaluation Criteria in Solid Tumors (RECIST) using diagnostic contrast-enhanced CT at 12 wk, with results available in 48 of the 53 patients. Overall survival (OS), progression-free survival (PFS), and local PFS (LPFS) or time to last censoring was recorded from the date of the PET scan. Data were abstracted by a single oncologist investigator who had previous experience with similar oncology study data collection and was masked to the PET results before data collection. OS was defined as the time in months between the PET scan and the date of death, PFS as time between the PET scan and locoregional or distant relapse, and LPFS as the time between the PET scan and locoregional relapse. Patients who were alive were censored at the time of the last clinical follow-up.

$^{18}$F-FDG PET/CT scans were all acquired using the same protocol in the same institution on either a Discovery VCT or a Discovery DST (both GE Healthcare), which were cross-calibrated to within 3% (*24*). Patients fasted for at least 6 h before the administration of 350–400 MBq of $^{18}$F-FDG. Ninety minutes after injection, scans were acquired from the upper thigh to the base of skull. Images were reconstructed using ordered-subset expectation maximization with a slice thickness of 3.27 mm and a pixel size of 5 mm. The CT component of the scans was acquired at 120 kVp and 65 mAs without the administration of an oral or intravenous contrast agent.

SUVmean, SUVmax, and SUVpeak (*25*), as well as MTV and TLG (SUVmean × MTV), were calculated for the primary tumors using semiautomated software for volume-of-interest (VOI) placement (Gold 3; Hermes). An initial threshold of 45% was applied for automated definition of volumes of interest and adjusted by the operator if nontumoral tissues were incorrectly included in the volume of interest by the software (*26*). Nodal disease was not included in the analysis. For purposes of textural analysis, regions of interest were drawn manually around the active primary tumors on each transaxial slice on which the tumor was visible. One observer with more than 15 y of experience with $^{18}$F-FDG PET in NSCLC and region-of-interest definition performed the analyses and was masked to the patient outcome data before analysis. Primary tumor texture was measured by coarseness, contrast, busyness, and complexity derived from 3-dimensional matrices, and differences between each PET image voxel and its neighbor were calculated, taking into consideration the neighboring voxels in the 2 adjacent planes for each voxel, as previously described (*19,22*). Reproducibility for $^{18}$F-FDG PET textural features in NSCLC has previously been reported as being as good as or better than that for SUVs (*27*).

Statistical analyses were performed using a software package (SPSS Statistics, version 20; IBM). A sample size calculation was not made for this retrospective cohort study, and corrections for multiple comparisons were not used. Differences in coarseness, contrast, busyness, and complexity, as well as differences in each of the SUV parameters, MTV, and TLG, were compared in nonresponders (stable disease/progressive disease) and responders (complete response/partial response) by CT RECIST with the Mann–Whitney *U* test. Areas under the receiver-operating-characteristic (ROC) curves were calculated for the textural features and the SUV parameters to assess the accuracy in predicting response according to RECIST.

Differences in Kaplan–Meier survival curves were evaluated using a nonparametric log-rank test. An optimum cut point for the level of the textural features was calculated, maximizing the sum of sensitivity and specificity from ROC curves, and was used to compare groups with either high or low textural values. Estimates of the sensitivity and specificity were calculated at this cut point, along with corresponding exact binomial confidence intervals (CIs). Cox regression was used to examine the effects of the textural parameters and other variables on the survival outcomes. Initially, the individual effect of each variable on the outcomes

was examined in a series of univariable analyses. Subsequently, a multivariable analysis was performed to jointly examine the variables. Because of the relatively small number of events, the multivariable analysis was restricted to variables with univariable $P$ values of less than 0.25. In addition, because of a highly skewed distribution of TLG, this variable was analyzed on the log scale. Furthermore, SUVmean and SUVmax, which are highly correlated with SUVpeak, and MTV, which is highly correlated with TLG, were not included in the regression analyses. Log–log plots were used to visually examine whether the proportional hazards assumptions were met. $P$ values of less than 0.05 were considered statistically significant, and 95% CIs were calculated.

## RESULTS

The demographic and clinical characteristics of patients are summarized in Table 1. The distribution of the SUV, MTV, TLG, and textural parameters is summarized in Table 2.

### Response Prediction

None of the SUV parameters, MTV, or TLG was significantly different between responders (partial response/complete response) and nonresponders (stable disease/progressive disease). RECIST responders showed statistically significantly lower coarseness and higher contrast and

### TABLE 1
Patient Demographic and Clinical Characteristics

| Patient characteristic | Value |
|---|---|
| Sex (n) | |
|   Male | 31 (58%) |
|   Female | 22 (42%) |
| Histology (n) | |
|   Adenocarcinoma | 21 (40%) |
|   Squamous cell carcinoma | 24 (45%) |
|   Not specified | 8 (15%) |
| T stage (n) | |
|   T1 | 6 (11%) |
|   T2 | 14 (27%) |
|   T3 | 15 (28%) |
|   T4 | 17 (32%) |
|   TX | 1 (2%) |
| N stage (n) | |
|   N0 | 11 (21%) |
|   N1 | 4 (8%) |
|   N2 | 33 (62%) |
|   N3 | 5 (9%) |
| Tumor stage (n) | |
|   IB | 3 (6%) |
|   IIB | 5 (9%) |
|   IIIA | 24 (45%) |
|   IIIB | 21 (40%) |
| Median duration between PET and treatment (d) | 45 (range, 0–174) |
| Median radiotherapy dose (Gy) | 64 (range, 55–64) |
| Median chemotherapy cycles (n) | 4 (range, 1–6) |

### TABLE 2
Range, Mean, and SD of SUV Parameters, MTV, TLG, and Measured Textural Features

| Parameter | Range | Mean | SD |
|---|---|---|---|
| SUVmean | 2.9–19.2 | 10.6 | 4.1 |
| SUVmax | 5.7–46.5 | 20.0 | 7.6 |
| SUVpeak | 4.2–42.3 | 16.7 | 6.8 |
| MTV (cm$^3$) | 2.2–519.0 | 54.7 | 76.5 |
| TLG (cm$^3$) | 8.2–5,656.0 | 588.9 | 829.7 |
| Coarseness | 0.0006–0.096 | 0.016 | 0.02 |
| Contrast | 0.0009–0.37 | 0.091 | 0.07 |
| Busyness | 0.092–2.77 | 0.65 | 0.57 |
| Complexity | 763–4,003 | 1,868 | 780 |

busyness than nonresponders, but no statistical difference was seen for complexity (Table 3).

The areas under the ROC curves for the ability to predict RECIST response for the textural features were 0.8 for coarseness (CI, 0.67–0.92; $P = 0.003$), 0.82 for contrast (CI, 0.7–0.94; $P = 0.002$), 0.72 for busyness (CI, 0.57–0.89; $P = 0.027$), and 0.54 for complexity (CI, 0.32–0.75; $P = 0.71$). Details are recorded in Table 4 and Figure 1. No significant differences from the line of reference were seen for any of the SUV parameters, MTV, or TLG.

### Survival Prediction

Median follow-up was for 21.2 mo (range, 2.1–51.1 mo). Median OS was 25.6 mo (range, 3.1–51.1 mo), PFS was 16.6 mo (range, 2.8–44.9 mo), and LPFS was not reached (range, 4.3–46 mo). By Kaplan–Meier analysis, OS, PFS, and LPFS were lower in patients with high primary tumor coarseness (median, 21.1 mo vs. not reached, $P = 0.003$; 12.6 vs. 25.8 mo, $P = 0.002$; and 12.9 vs. 20.5 mo, $P = 0.016$, respectively) (Figs. 2A–2C).

Contrast and busyness did not show significant associations with OS ($P = 0.075$ and 0.059, respectively), but PFS and LPFS were significantly longer in patients with high levels of each (for contrast: median of 20.5 vs. 12.6 mo, $P = 0.015$, and median not reached vs. 24 mo, $P = 0.02$; and for busyness: median of 20.5 vs. 12.6 mo, $P = 0.01$, and median not reached vs. 24 mo, $P = 0.006$) (Figs. 2D–2I) (Table 5). Neither complexity nor any of the SUV parameters showed statistically significant associations with the survival parameters.

The results of univariable and multivariable Cox regression analysis, used to examine the effects of textural parameters and other variables on survival outcomes, are shown in Table 6. The log–log plots suggested that the hazards were approximately proportional for all variables.

Coarseness was associated with OS in both the univariable and multivariable analyses ($P = 0.007$ and 0.02, respectively). A high coarseness was associated with an increased risk of death, and the hazard of death at any time was almost 5 times higher for patients with a high coarseness value than for those with lower values (from multivariable analysis).

**TABLE 3**
Mean Values for Calculated Textural Features for Responders and Nonresponders by CT RECIST

| Parameter | Responders (complete or partial response) | Nonresponders (stable or progressive disease) | P (Mann–Whitney U test) |
|---|---|---|---|
| Coarseness | 0.012 | 0.027 | 0.004 |
| Contrast | 0.110 | 0.044 | 0.002 |
| Busyness | 0.760 | 0.370 | 0.027 |
| Complexity | 1,938 | 1,926 | 0.706 |

For PFS, coarseness, contrast, and busyness were all statistically significant in the univariable analyses ($P = 0.003, 0.02$, and $0.02$, respectively). High coarseness values were associated with an increased risk of progression, whereas high contrast and busyness values were associated with a lower risk of progression. The multivariable analyses suggested that no variables were statistically significant. Of the texture variables, the largest effects were for coarseness.

Coarseness was found to be most associated with LPFS. High coarseness values were associated with a greater risk of local progression and thus shorter times to local progression. This result was statistically significant in the univariable analyses ($P = 0.01$), with the result of borderline statistical significance in the multivariable analyses ($P = 0.06$).

## DISCUSSION

Our results add to the accumulating evidence that measurements of textural features of $^{18}$F-FDG uptake within PET images of cancer can predict response and are associated with survival. To our knowledge, this has not previously been reported in patients with NSCLC undergoing concurrent chemoradiotherapy. We also found that textural features performed better than SUV parameters, MTV, and TLG, which had no predictive or prognostic power in this series. The ineffectiveness of these parameters was possibly due to poorer discrimination in a group of pre-

**TABLE 4**
Area Under ROC Curves for Ability of Measured Textural Features, SUV Parameters, MTV, and TLG to Predict Response Using RECIST

| Parameter | Area under ROC curve | 95% CI | P |
|---|---|---|---|
| Coarseness | 0.80 | 0.67–0.92 | 0.003 |
| Contrast | 0.82 | 0.70–0.94 | 0.002 |
| Busyness | 0.72 | 0.57–0.89 | 0.027 |
| Complexity | 0.54 | 0.32–0.75 | 0.71 |
| SUVmean | 0.59 | 0.38–0.79 | 0.39 |
| SUVmax | 0.67 | 0.47–0.84 | 0.12 |
| SUVpeak | 0.64 | 0.46–0.83 | 0.16 |
| MTV | 0.65 | 0.45–0.85 | 0.135 |
| TLG | 0.68 | 0.51–0.85 | 0.07 |
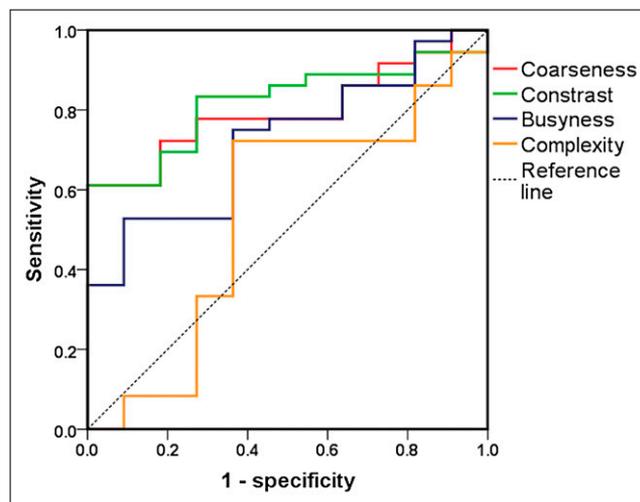


**FIGURE 1.** ROC curves for baseline $^{18}$F-FDG PET primary tumor coarseness, contrast, busyness, and complexity for identification of responders vs. nonresponders by RECIST at 12 wk. Table 4 shows areas under ROC curve.

dominantly higher-stage patients and those with comorbidity, resulting in their being selected for chemoradiotherapy rather than surgery. Specifically, the textural features derived from NGTDMs—including coarseness, contrast, and busyness—were able to differentiate subsequent responders from nonresponders. All 3 features were related to PFS and LPFS, whereas coarseness was also related to OS and was an independent predictor of survival parameters, compared with other potential clinical and imaging risk factors.

The ability to predict response and survival from pretreatment scans is an advantage over using serial scans, and textural analysis has the benefit of being a postprocessing technique that can be applied to data acquired during standard clinical imaging protocols, maximizing the information that can be derived from standard PET images. Baseline assessment is particularly advantageous in lung cancer being treated with radiotherapy because much of the posttreatment $^{18}$F-FDG activity may be due to pneumonitis rather than residual cancer, thus making interpretation and quantitative response assessment problematic with PET (28).

Coarseness, contrast, busyness, and complexity are fundamental parameters of image texture that have been correlated with human perception of texture within an image (18,22). These features are derived from NGTDMs. They describe local tumor texture based on differences between each voxel and the neighboring voxels in adjacent image planes. Coarseness has been likened to granularity within an image and is the most fundamental property of texture. One study of esophageal carcinoma (19) described coarseness as a feature that may discriminate responders to chemoradiotherapy from nonresponders, although contrast and busyness were not predictive in that study. Coarseness is also a parameter that best differentiates head and neck cancer primary and nodal tumors from normal tissues (18)
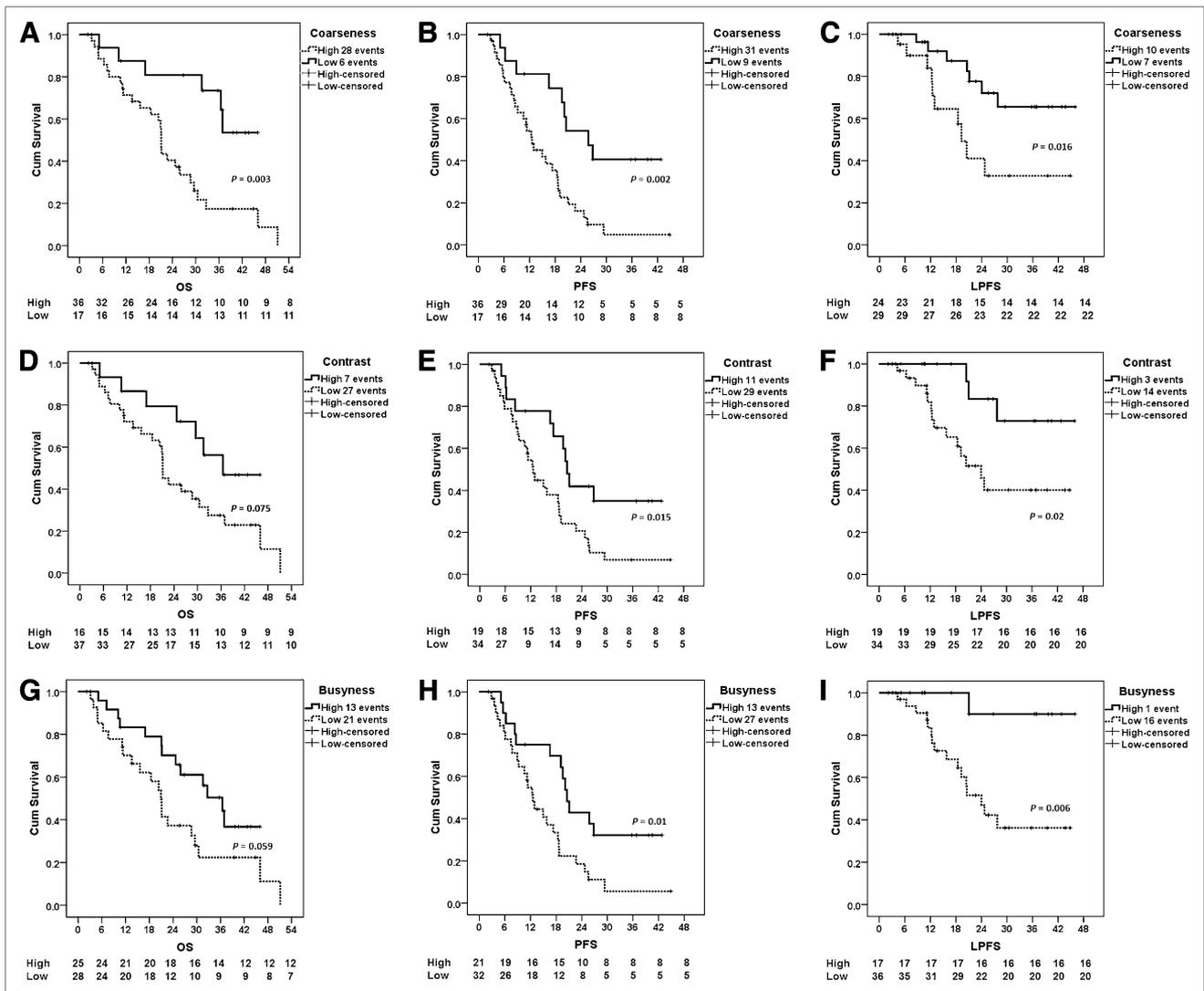
**FIGURE 2.** Kaplan–Meier plots demonstrating differences in patients with high and low primary tumor $^{18}$F-FDG PET coarseness (A–C), contrast (D–F), and busyness (G–I). Differences in OS (A, D, and G), PFS (B, E, and H), and LPFS (C, F, and I) are demonstrated. Cum = cumulative.

and in combination with other textural features has been used to delineate radiotherapy planning volumes in head and neck cancer (*17*). Contrast relates to the dynamic range of intensity levels in an image, and the level of local intensity variation and busyness relates to the rate of intensity change within an image. Complexity relates to high information content—for example, when there are many sharp edges or lines—but may be more relevant to 2-dimensional images.

Other textural features of $^{18}$F-FDG PET images have been reported to be predictive and prognostic. In sarcoma, the measurement of heterogeneity, by variation from a model for homogeneous tissues, has been described and predicts patient outcome (*15*), and regional textural features predicted response to chemoradiotherapy in esophageal carcinoma (*19*).

There is also accumulating literature on the predictive abilities of several textural features in morphologic imaging

methods, including CT and MRI. For example, changes in textural features related to the heterogeneity of CT images have been found to be independent predictors of time to progression in renal carcinomas treated with tyrosine kinase inhibitors (*29*), and textural features in unenhanced CT scans of esophageal carcinoma have been related to SUV parameters in corresponding $^{18}$F-FDG PET scans and to tumor stage and survival (*30*). Specifically in lung cancer, CT features have been shown to help differentiate aggressive from nonaggressive NSCLC (*31*) and to show differences between histologic subtypes (*32*). More recent work has shown relationships between CT features and survival (*33*), glucose metabolism (*34*), and histologic correlations including angiogenic and hypoxia markers (*35*).

Although several textural features in structural and functional imaging of cancer have been shown to differentiate tumor types, predict treatment response, or be

**TABLE 5**
Data Related to Kaplan–Meier Analysis

| Parameter | Patients per group | | Events per group | | Kaplan–Meier χ² | | Sensitivity at optimal cutoff | Specificity at optimal cutoff |
|---|---|---|---|---|---|---|---|---|
| | High | Low | High | Low | Log rank | P | | |
| **Coarseness** | | | | | | | | |
| OS | 36 | 17 | 29 | 6 | 8.90 | 0.003 | 0.82 (0.65–0.93) | 0.58 (0.33–0.80) |
| PFS | 36 | 17 | 31 | 9 | 9.54 | 0.002 | 0.78 (0.62–0.89) | 0.62 (0.32–0.86) |
| LPFS | 24 | 29 | 10 | 7 | 5.77 | 0.016 | 0.59 (0.32–0.82) | 0.61 (0.43–0.77) |
| **Contrast** | | | | | | | | |
| OS | 16 | 37 | 7 | 27 | 3.18 | 0.075 | 0.79 (0.62–0.91) | 0.47 (0.24–0.71) |
| PFS | 19 | 34 | 11 | 29 | 5.96 | 0.015 | 0.73 (0.56–0.85) | 0.62 (0.32–0.86) |
| LPFS | 19 | 34 | 3 | 14 | 5.40 | 0.02 | 0.82 (0.57–0.96) | 0.44 (0.28–0.62) |
| **Busyness** | | | | | | | | |
| OS | 25 | 28 | 13 | 21 | 3.55 | 0.059 | 0.62 (0.44–0.78) | 0.63 (0.38–0.84) |
| PFS | 21 | 32 | 13 | 27 | 6.60 | 0.01 | 0.68 (0.51–0.81) | 0.62 (0.32–0.86) |
| LPFS | 17 | 36 | 1 | 16 | 7.44 | 0.006 | 0.94 (0.71–1.00) | 0.44 (0.28–0.62) |
| **Complexity** | | | | | | | | |
| OS | 18 | 35 | 10 | 24 | 1.94 | 0.16 | 0.71 (0.53–0.85) | 0.42 (0.20–0.67) |
| PFS | 29 | 24 | 24 | 16 | 2.67 | 0.61 | 0.60 (0.43–0.75) | 0.62 (0.32–0.86) |
| LPFS | 31 | 22 | 13 | 4 | 0.95 | 0.33 | 0.76 (0.50–0.93) | 0.50 (0.33–0.67) |

Data in parentheses are 95% CIs.

associated with survival, the biologic correlates of textural features are largely unknown. It is postulated that increased image heterogeneity within tumors may be associated with differences in regional tumor cellularity, proliferation, hypoxia, angiogenesis, and necrosis (19,35), factors that independently have been associated with more aggressive behavior, poorer response to treatment, and worse prognosis. Although it is unlikely that structural and functional imaging textural features are associated with the same biologic causes of spatial intensity variations within an image, in general, features that correspond to increased heterogeneity have been assumed to relate to a poorer prognosis and poor response to treatment. However, given the multitude of textural parameters that have been described and the complexities resulting from the measurement of local, regional, or global textural features, this assumption is probably an oversimplification of the relationships between tumor biology and heterogeneity within an image. For example, CT features related to increased heterogeneity, including increased entropy or decreased uniformity, predict poor response or survival (29,30,33). On the other hand, in ^{18}F-FDG PET of esophageal carcinoma, responders to treatment showed greater local heterogeneity at baseline, but measures of regional tumor heterogeneity showed better response stratification (19). In head and neck cancer, tumor and nodes have been reported as having low coarseness and busyness but high contrast, compared with normal tissues (18). The relationship between textural features and tissue characteristics is therefore complex, and textural feature measurements can clearly not simply be regarded as lying on a spectrum between heterogeneity and homogeneity. Thus, there is a need to carefully investigate textural

features from different imaging modalities and to use different PET tracers to correlate with histopathologic features that may influence image texture, including angiogenesis, hypoxia, and proliferation, either in a preclinical model or in humans when tissue is available for complementary histologic analysis.

Our study is limited by being retrospective. There was some heterogeneity in the stage and histology between patients, although the study benefits from a homogeneous treatment regime in the cohort of patients. Though the results would appear promising for new predictive biomarkers, caution should be exercised until the results can be confirmed prospectively. Tumor regions of interest for textural analysis were drawn manually, and it is possible that better inter- and intraobserver variation would be gained if automated methods were used, particularly for multicenter studies in the future. There will also be a need to understand how data from different scanners at different centers might vary for these methods to become of utility in a multicenter setting.

## CONCLUSION

Abnormal texture in baseline ^{18}F-FDG PET scans, as measured by coarseness, contrast, and busyness, in patients with NSCLC is associated with nonresponse to chemoradiotherapy by RECIST and with poorer prognosis. In conjunction with other similar studies, this association suggests that textural image features may provide predictive and prognostic biomarkers that offer promise for personalized medicine in which patients might be stratified before treatment in clinical trials and in clinical practice, with the potential to reduce toxicity from ineffective treatments.

**TABLE 6**
Effects of Variables on OS, PFS, and LPFS

| Characteristic | OS Univariable HR | P | OS Multivariable HR | P | PFS Univariable HR | P | PFS Multivariable HR | P | LPFS Univariable HR | P | LPFS Multivariable HR | P |
|---|---|---|---|---|---|---|---|---|---|---|---|---|
| Age* | 1.26 (0.86–1.83) | 0.23 | 1.43 (0.95–2.17) | 0.09 | 1.03 (0.74–1.44) | 0.85 | | | 0.84 (0.50–1.39) | 0.49 | | |
| Male sex | 1.13 (0.56–2.28) | 0.73 | | | 1.29 (0.68–2.46) | 0.44 | | | 0.94 (0.36–2.48) | 0.90 | | |
| Stage 1 or 2 | 1 | 0.42 | | | 1 | 0.81 | | | 1 | 0.64 | | |
| Stage 3a | 0.90 (0.32–2.56) | | | | 1.38 (0.51–3.72) | | | | 1.67 (0.36–7.70) | | | |
| Stage 3b | 1.47 (0.52–4.16) | | | | 1.28 (0.47–3.49) | | | | 1.06 (0.21–5.49) | | | |
| Squamous cell carcinoma histology | 1.04 (0.48–2.26) | 0.91 | | | 0.86 (0.44–1.69) | 0.67 | | | 0.57 (0.19–1.75) | 0.33 | | |
| SUVpeak† | 0.87 (0.63–1.18) | 0.36 | | | 0.87 (0.65–1.16) | 0.34 | | | 0.82 (0.54–1.24) | 0.35 | | |
| TLG‡ | 0.93 (0.72–1.21) | 0.59 | | | 0.82 (0.64–1.05) | 0.11 | 1.06 (0.74–1.51) | 0.76 | 0.73 (0.53–0.99) | 0.04 | 0.91 (0.59–1.41) | 0.68 |
| High coarseness | 3.48 (1.41–8.63) | 0.007 | 4.86 (1.32–17.9) | 0.02 | 3.18 (1.48–6.85) | 0.003 | 2.41 (0.82–7.09) | 0.11 | 6.69 (1.50–29.8) | 0.01 | 5.56 (0.90–34.1) | 0.06 |
| High contrast | 0.47 (0.20–1.10) | 0.08 | 1.11 (0.41–2.99) | 0.84 | 0.40 (0.19–0.85) | 0.02 | 0.60 (0.24–1.48) | 0.27 | 0.30 (0.09–1.07) | 0.07 | 0.67 (0.16–1.48) | 0.58 |
| High busyness | 0.51 (0.25–1.04) | 0.06 | 1.12 (0.44–2.92) | 0.80 | 0.46 (0.24–0.88) | 0.02 | 0.97 (0.37–2.53) | 0.95 | 0.36 (0.13–0.98) | 0.05 | 1.18 (0.32–2.53) | 0.80 |
| High complexity | 0.59 (0.28–1.25) | 0.17 | 1.11 (0.43–2.87) | 0.82 | 0.61 (0.32–1.18) | 0.17 | 0.87 (0.40–1.92) | 0.73 | 0.60 (0.22–1.62) | 0.31 | | |

*Hazard ratios are reported for 10-unit increase in variable.
†Hazard ratios are reported for 5-unit increase in variable.
‡Variable was analyzed on log scale.
Figures reported are hazard ratios and corresponding 95% CIs. For variables measured on continuous scale, hazard ratios are reported for 1-unit increase in that variable (unless otherwise indicated). Data in parentheses are 95% CIs.

## REFERENCES

1. Yoon DH, Baek S, Choi CM, et al. FDG-PET as a potential tool for selecting patients with advanced non-small cell lung cancer who may be spared maintenance therapy after first-line chemotherapy. *Clin Cancer Res.* 2011;17:5093–5100.
2. Shiraishi K, Nomori H, Ohba Y, et al. Repeat FDG-PET for predicting pathological tumor response and prognosis after neoadjuvant treatment in nonsmall cell lung cancer: comparison with computed tomography. *Ann Thorac Cardiovasc Surg.* 2010;16:394–400.
3. Rebollo-Aguirre AC, Ramos-Font C, Villegas Portero R, et al. Is FDG-PET suitable for evaluating neoadjuvant therapy in non-small cell lung cancer? Evidence with systematic review of the literature. *J Surg Oncol.* 2010;101:486–494.
4. Lee DH, Kim SK, Lee HY, et al. Early prediction of response to first-line therapy using integrated 18F-FDG PET/CT for patients with advanced/metastatic non-small cell lung cancer. *J Thorac Oncol.* 2009;4:816–821.
5. Dooms C, Verbeken E, Stroobants S, et al. Prognostic stratification of stage IIIA-N2 non-small-cell lung cancer after induction chemotherapy: a model based on the combination of morphometric-pathologic response in mediastinal nodes and primary tumor response on serial 18-fluoro-2-deoxy-glucose positron emission tomography. *J Clin Oncol.* 2008;26:1128–1134.
6. de Geus-Oei LF, van der Heijden HF, Visser EP, et al. Chemotherapy response evaluation with 18F-FDG PET in patients with non-small cell lung cancer. *J Nucl Med.* 2007;48:1592–1598.
7. Mac Manus MP, Hicks RJ, Matthews JP, et al. Metabolic (FDG-PET) response after radical radiotherapy/chemoradiotherapy for non-small cell lung cancer correlates with patterns of failure. *Lung Cancer.* 2005;49:95–108.
8. Huang W, Zhou T, Ma L, et al. Standard uptake value and metabolic tumor volume of 18F-FDG PET/CT predict short-term outcome early in the course of chemoradiotherapy in advanced non-small cell lung cancer. *Eur J Nucl Med Mol Imaging.* 2011;38:1628–1635.
9. O'Brien ME, Myerson JS, Coward JI, et al. A phase II study of 18F-fluorodeoxyglucose PET-CT in non-small cell lung cancer patients receiving erlotinib (Tarceva); objective and symptomatic responses at 6 and 12 weeks. *Eur J Cancer.* 2012;48:68–74.
10. Memon AA, Weber B, Winterdahl M, et al. PET imaging of patients with non-small cell lung cancer employing an EGF receptor targeting drug as tracer. *Br J Cancer.* 2011;105:1850–1855.
11. Ohno Y, Koyama H, Yoshikawa T, et al. Diffusion-weighted MRI versus 18F-FDG PET/CT: performance as predictors of tumor treatment response and patient survival in patients with non-small cell lung cancer receiving chemoradiotherapy. *AJR.* 2012;198:75–82.
12. Zhang HQ, Yu JM, Meng X, et al. Prognostic value of serial [18F]fluorodeoxyglucose PET-CT uptake in stage III patients with non-small cell lung cancer treated by concurrent chemoradiotherapy. *Eur J Radiol.* 2011;77:92–96.
13. Borst GR, Belderbos JS, Boellaard R, et al. Standardised FDG uptake: a prognostic factor for inoperable non-small cell lung cancer. *Eur J Cancer.* 2005;41:1533–1541.
14. Lee KH, Lee SH, Kim DW, et al. High fluorodeoxyglucose uptake on positron emission tomography in patients with advanced non-small cell lung cancer on platinum-based combination chemotherapy. *Clin Cancer Res.* 2006;12:4232–4236.
15. Eary JF, O'Sullivan F, O'Sullivan J, Conrad EU. Spatial heterogeneity in sarcoma 18F-FDG uptake as a predictor of patient outcome. *J Nucl Med.* 2008;49:1973–1979.
16. El Naqa I, Grigsby PW, Aptea A, et al. Exploring feature-based approaches in PET images for predicting cancer treatment outcomes. *Pattern Recognit.* 2009;42:1162–1171.
17. Yu H, Caldwell C, Mah K, et al. Automated radiation targeting in head-and-neck cancer using region-based texture analysis of PET and CT images. *Int J Radiat Oncol Biol Phys.* 2009;75:618–625.
18. Yu H, Caldwell C, Mah K, Mozeg D. Coregistered FDG PET/CT-based textural characterization of head and neck cancer for radiation treatment planning. *IEEE Trans Med Imaging.* 2009;28:374–383.
19. Tixier F, Le Rest CC, Hatt M, et al. Intratumor heterogeneity characterized by textural features on baseline 18F-FDG PET images predicts response to concomitant radiochemotherapy in esophageal cancer. *J Nucl Med.* 2011;52:369–378.
20. van Velden FH, Cheebsumon P, Yaqub M, et al. Evaluation of a cumulative SUV-volume histogram method for parameterizing heterogeneous intratumoural FDG uptake in non-small cell lung cancer PET studies. *Eur J Nucl Med Mol Imaging.* 2011;38:1636–1647.
21. Vaidya M, Creach KM, Frye J, et al. Combined PET/CT image characteristics for radiotherapy tumor response in lung cancer. *Radiother Oncol.* 2012;102:239–245.
22. Amadasun M, King R. Textural features corresponding to textural properties. *IEEE Trans Syst Man Cybern.* 1989;19:1264–1274.
23. Goldstraw P, Crowley J, Chansky K, et al. The IASLC Lung Cancer Staging Project: proposals for the revision of the TNM stage groupings in the forthcoming (seventh) ed. of the TNM Classification of malignant tumours. *J Thorac Oncol.* 2007;2:706–714.
24. Schleyer PJ, Baker S, Barrington SF, et al. Establishment of acquisition and reconstruction parameters for a GE Discovery VCT PET-CT scanner. *Eur J Nucl Med Mol Imaging.* 2008;35:S340–S341.
25. Wahl RL, Jacene H, Kasamon Y, Lodge MA. From RECIST to PERCIST: evolving considerations for PET response criteria in solid tumors. *J Nucl Med.* 2009;50:122S–150S.
26. Uto F, Shiba E, Onoue S, et al. Phantom study on radiotherapy planning using PET/CT–delineation of GTV by evaluating SUV. *J Radiat Res (Tokyo).* 2010;51:157–164.
27. Tixier F, Hatt M, Cheze Le Rest C, et al. Reproducibility of tumor uptake heterogeneity characterisation through textural feature analysis in 18F-FDG PET. *J Nucl Med.* 2012;53:693–700.
28. Wiegman EM, Pruim J, Ubbels JF, et al. 18F-FDG PET during stereotactic body radiotherapy for stage I lung tumours cannot predict outcome: a pilot study. *Eur J Nucl Med Mol Imaging.* 2011;38:1059–1063.
29. Goh V, Ganeshan B, Nathan P, et al. Assessment of response to tyrosine kinase inhibitors in metastatic renal cell cancer: CT texture as a predictive biomarker. *Radiology.* 2011;261:165–171.
30. Ganeshan B, Skogen K, Pressney I, et al. Tumour heterogeneity in oesophageal cancer assessed by CT texture analysis: preliminary evidence of an association with tumour metabolism, stage, and survival. *Clin Radiol.* 2012;67:157–164.
31. Al-Kadi OS, Watson D. Texture analysis of aggressive and nonaggressive lung tumor CE CT images. *IEEE Trans Biomed Eng.* 2008;55:1822–1830.
32. Kido S, Kuriyama K, Higashiyama M, et al. Fractal analysis of internal and peripheral textures of small peripheral bronchogenic carcinomas in thin-section computed tomography: comparison of bronchioloalveolar cell carcinomas with non bronchioloalveolar cell carcinomas. *J Comput Assist Tomogr.* 2003;27:56–61.
33. Ganeshan B, Panayiotou E, Burnand K, et al. Tumour heterogeneity in non-small cell lung carcinoma assessed by CT texture analysis: a potential marker of survival. *Eur Radiol.* 2012;22:796–802.
34. Ganeshan B, Abaleke S, Young RC, et al. Texture analysis of non-small cell lung cancer on unenhanced computed tomography: initial evidence for a relationship with tumour glucose metabolism and stage. *Cancer Imaging.* 2010;10:137–143.
35. Ganeshan B, Goh V, Mandeville H, et al. CT of non-small cell lung cancer: Histopathological correlates for texture parameters. *Radiology.* In press.